

Topic	Additional seismogram examples at distances beyond 100°
Authors	Klaus Klinge, Federal Institute for Geosciences and Natural Resources, Seismological Central Observatory, Gräfenberg (SZGRF), Mozartstrasse 57, 91052 Erlangen, Germany, Fax: +49 9131 8104 099, E-mail: klinge@szgrf.bgr.de Siegfried Wendt, Geophysical Observatory Collm, University of Leipzig, D-04779 Wermsdorf, Germany, E-mail: wendt@rz.uni-leipzig.de Peter Bormann (formerly GeoForschungsZentrum Potsdam, Telegrafenberg, 14473 Potsdam, Germany); E-mail: pb65@gmx.net
Version	October, 2002

Note: Most of the examples given below show either records of the German Regional Seismic Network (GRSN; aperture about 500 x 800 km) or of the Gräfenberg broadband array (GRF; aperture 45 x 110 km; see Figs. 8.14 and 9.4 in the manual Chapters 8 and 9, respectively). The following abbreviations have been used: OT – origin time in UT (universal time), D – epicentral distance in degrees, BAZ – backazimuth in degrees, h – focal depth in kilometer.

Example 1: Earthquake in the Chile-Bolivia border region (intermediate source depth)

USGS NEIC-data: 2002-03-08 OT 04:56:21.7 21.6S 68.2W h = 123 km Mw = 6.5;
The epicentral distances of the GRSN stations range between 97° < D < 103°.

Figures 1 a and b show enlarged sections of the recordings made of this intermediate depth earthquake at stations of the GRSN around the beginning of the shadow zone of the Earth's core (for the full records see Fig. 11.57 left). Figure 1a depicts the first 24 minutes of the long-period recordings (SRO-LP simulation) of the horizontal R and T components whereas Figure 1 b shows the related Z-component recordings of the first 8 min (lower part) and 17 min (upper part), respectively. The following diagnostic features can be recognized:

- Pdif is by far the smallest body-wave arrival, even in the vertical component, however, its SNR is still large enough for this medium-size earthquake in LP recordings;
- SKS (here also with its depth phase sSKS) forms the first strong shear-wave arrival, necessarily in the radial (R) horizontal component, whereas S (also with its depth phase sS) is a comparably strong later shear-wave arrival, here (however not always!) with large amplitudes in the transverse (T)-component records;
- SP (and its depth phase) is also (necessarily!) strongest in the R component whereas SS is frequently (not always! see Figure 2) strongest in the long-period T component;
- SKS and SP have also well developed onsets in Z-component LP records with amplitudes comparably strong or even larger than for Pdif and PP;
- Pdif and PP may also have well developed depth phases (here sPdif and sPP, respectively) in Z-component LP records;
- the missing of the depth phases pPdif and pPP in Figure 1b is due to the different P- and S-wave radiation pattern from a shear source (see Figs. 3.25 and 3.26) and the specific rupture orientation with respect to the seismic station in the considered case; this is not a general feature, rather pP, pPP etc. are often stronger;
- PP has, when compared with Pdif, a larger R component because of its larger incidence angle; and SP a larger Z component than PS.

2002-03-28 OT 04:56:21.7 h = 123 km Chile Bolivia border region

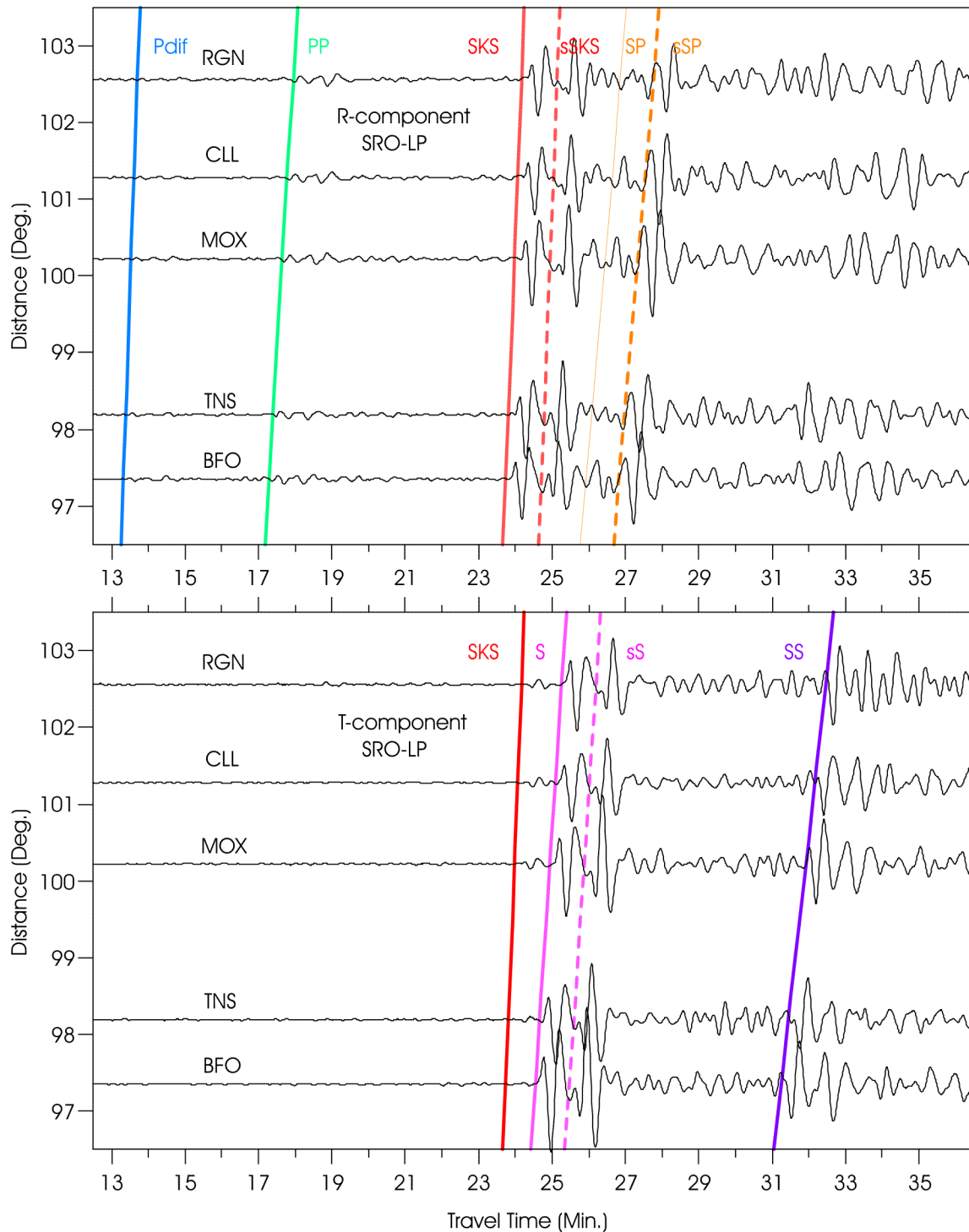


Figure 1a SRO-LP filtered BB records of GRSN stations. Upper traces: R component; lower traces: T component. Note that the phases SKS and SP, as well as their depth phases, have necessarily their largest horizontal amplitudes in the R component, as the longitudinal waves Pdif and PP. In contrast, S and SS may have their largest amplitudes in the T component, depending on the primary ratio of SV/SH energy radiated by the earthquake source.

2002-03-28 OT 04:56:21.7 h = 123 km Chile Bolivia border region

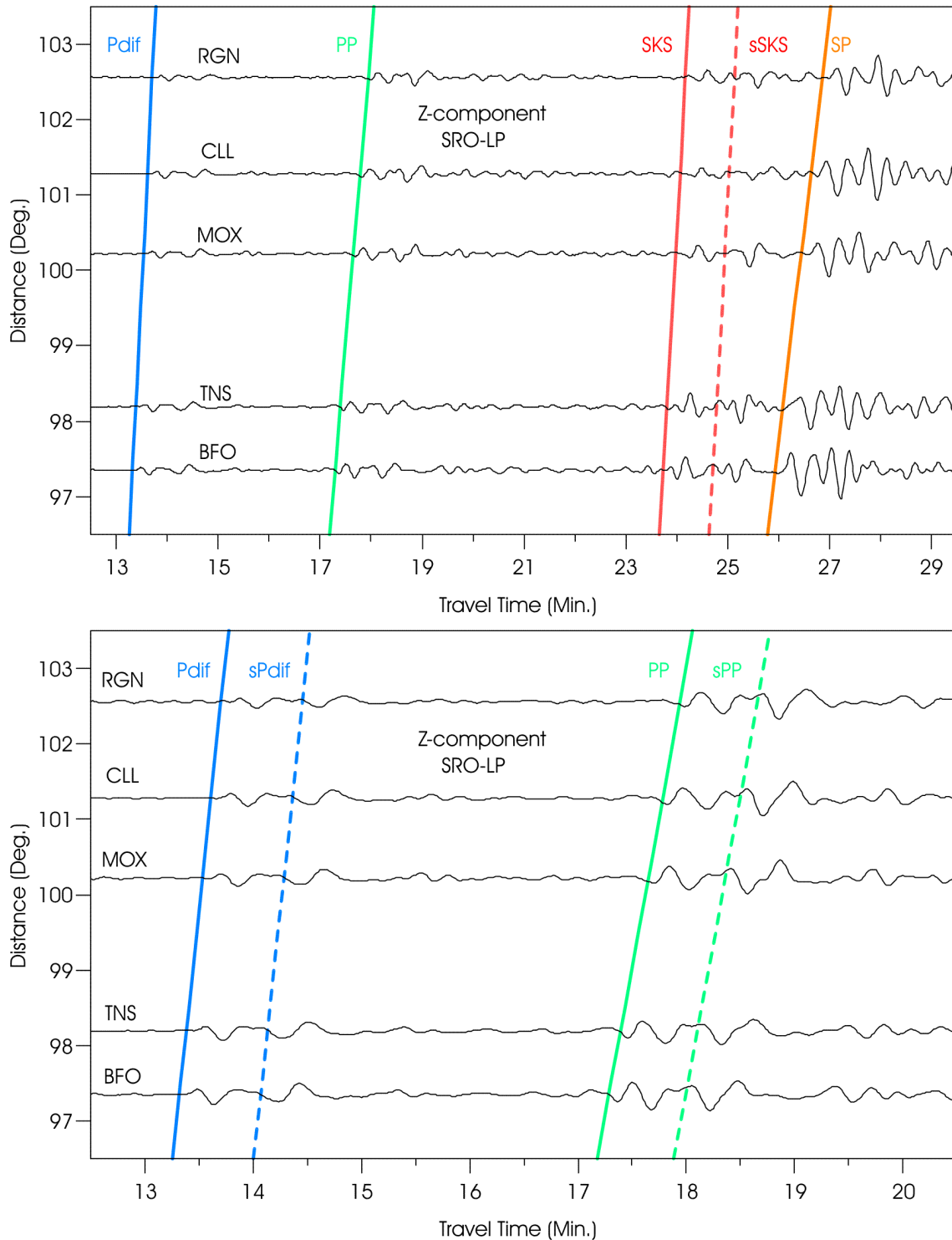


Figure 1b Enlarged vertical (Z)-component SRO-LP filtered BB records of GRSN stations shown in Figure 1a. Upper traces: Body-wave phases up to SP; lower traces: cut-out of the first 8 minutes of the record with longitudinal phases only. Note the well developed depth phases sPdif and sPP. The theoretically expected arrival times according to the IASP91 model (Kennett and Engdahl, 1991) have been inserted in both Figure 1a and b.

Example 2: Earthquake in the Mariana Islands region (intermediate source depth)

USGS NEIC-data: 2002-04-26 OT 16:06:06.8 13.1N 144.6E h = 85 km Mw = 7.1;
The epicentral distances of the GRSN stations range between $101^\circ < D < 108^\circ$.

The waves from this source at nearly the same distance as for the Chile-Bolivia earthquake approach the GRSN stations from nearly the opposite backazimuth (see Fig. 11.57), however, the general wave types and waveform features in different record components are nearly the same as Figure 1, with one exception: SS is best developed in the R component and there is no S wave visible in the T component, i.e., the shear-wave energy generated by this source was almost exclusively of SV type.

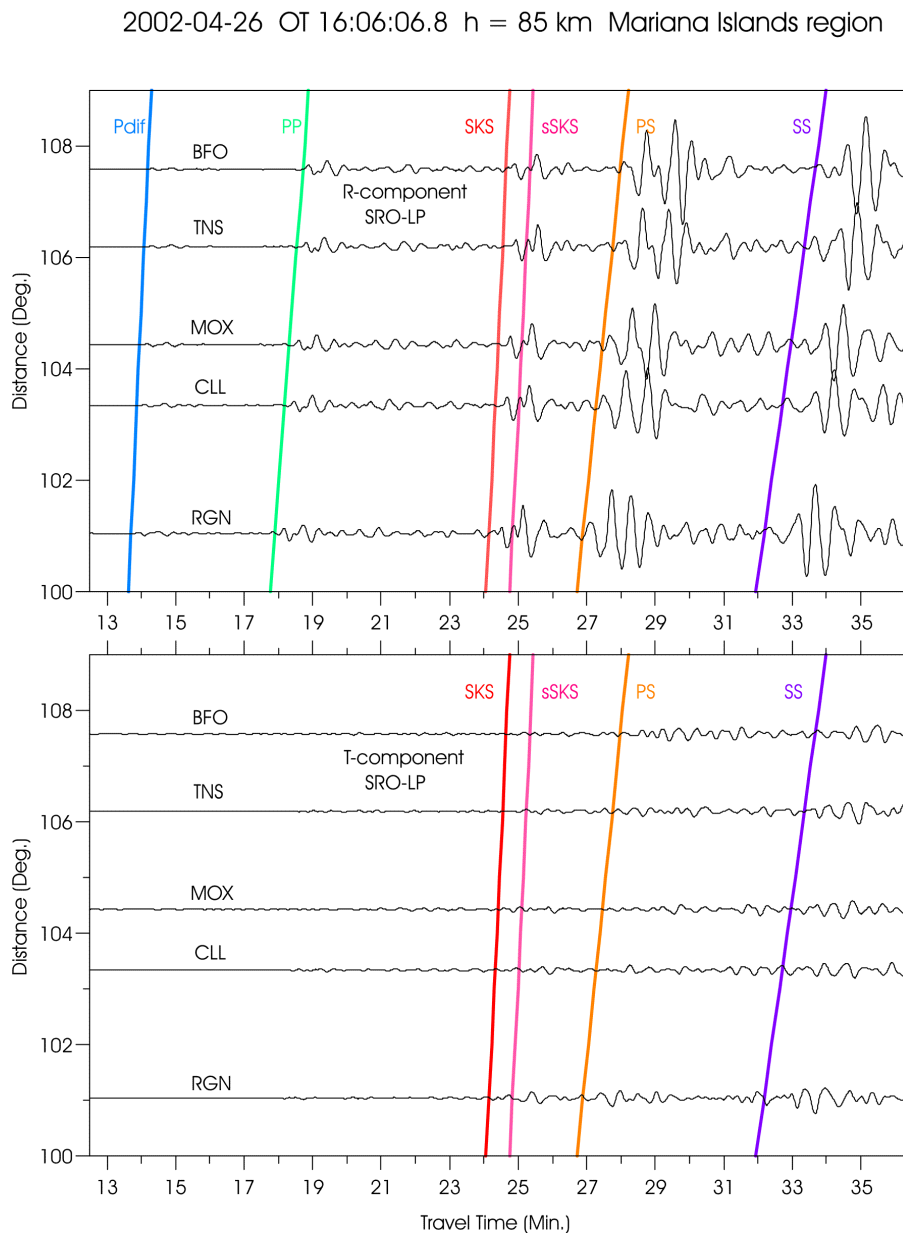


Figure 2a SRO-LP filtered BB records of GRSN stations. Upper traces: R component; lower traces: T component. Note that in these records PS has about four times larger amplitudes than SKS and all phases are not visible or rather weak in the T component.

2002-04-26 OT 16:06:06.8 h = 85 km Mariana Islands region

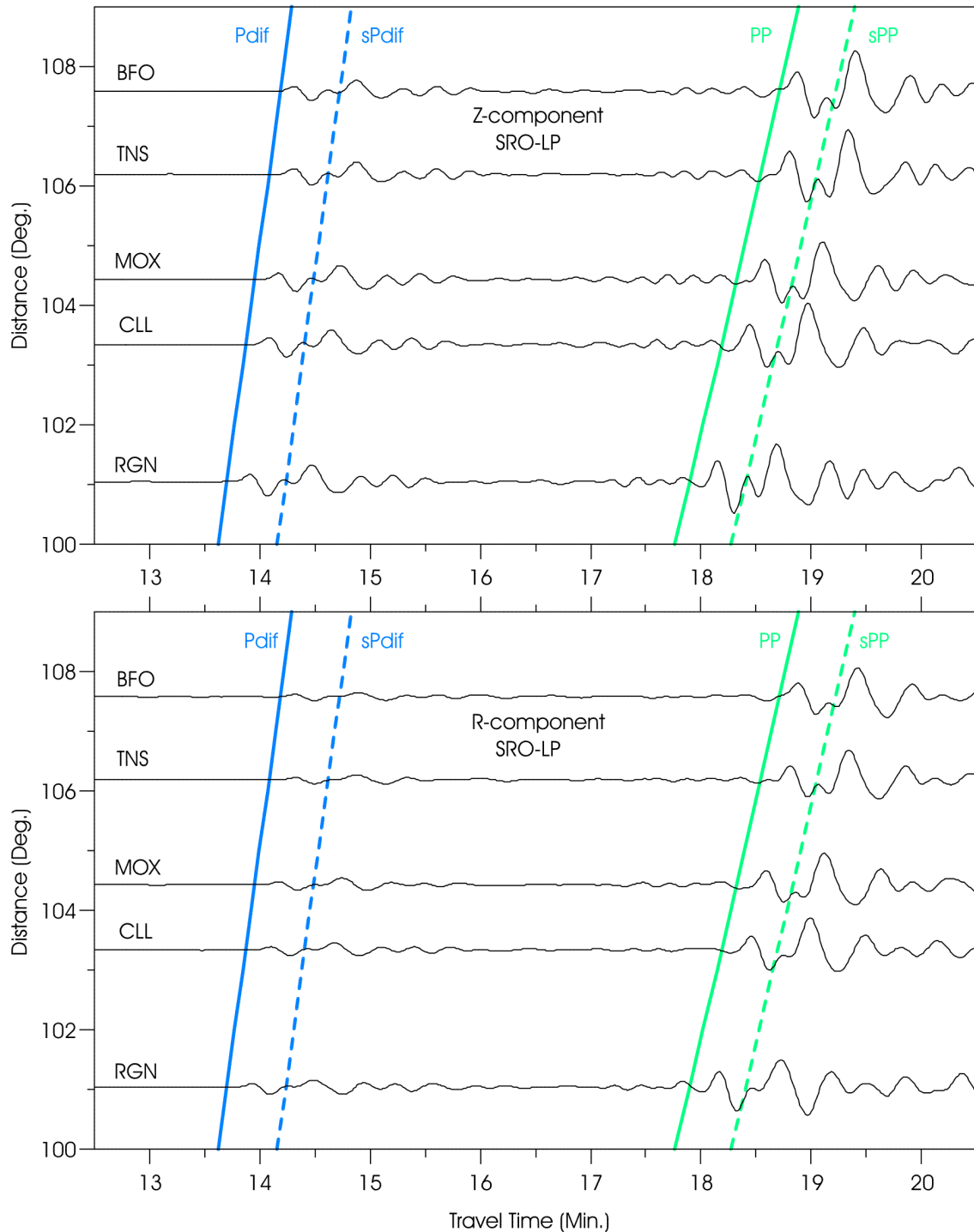


Figure 2b Enlarged cut-out of the SRO-LP filtered BB records of GRSN stations shown in Figure 2a. Upper traces: Z component; lower traces: R component. Note the well developed depth phases sPdif and sPP. The theoretically expected arrival times according to the IASP91 model (Kennett and Engdahl, 1991) have been inserted in both Figure 2a and b. Note that the amplitude ratio Z/R is larger than for Pdif than for PP because of the smaller (steeper) incidence angle of Pdif.

Example 3: Earthquake in the Banda Sea region (intermediate source depth) with phases PKPdif, PKKPab and PKKPbc

USGS NEIC-data: 2000-03-03 OT 22:09:13.5 7.313S 128.642E h = 148 km mb = 6.4;
(D =113° and BAZ =73.9° from GRF, h = 140 km)

Shown are various short-period filtered seismograms (WWSSN-SP simulation) recorded at GRSN-, GRF- and GEOFON-stations. All traces are sorted according to increasing epicentral distance within the range D = 110.8° (RUE) and 116.2° (WLF). Phases Pdif, PKiKP, PP, SP, PKKPbc and PKKPab are shown. Additionally, ray-paths and travel-time curves are presented.

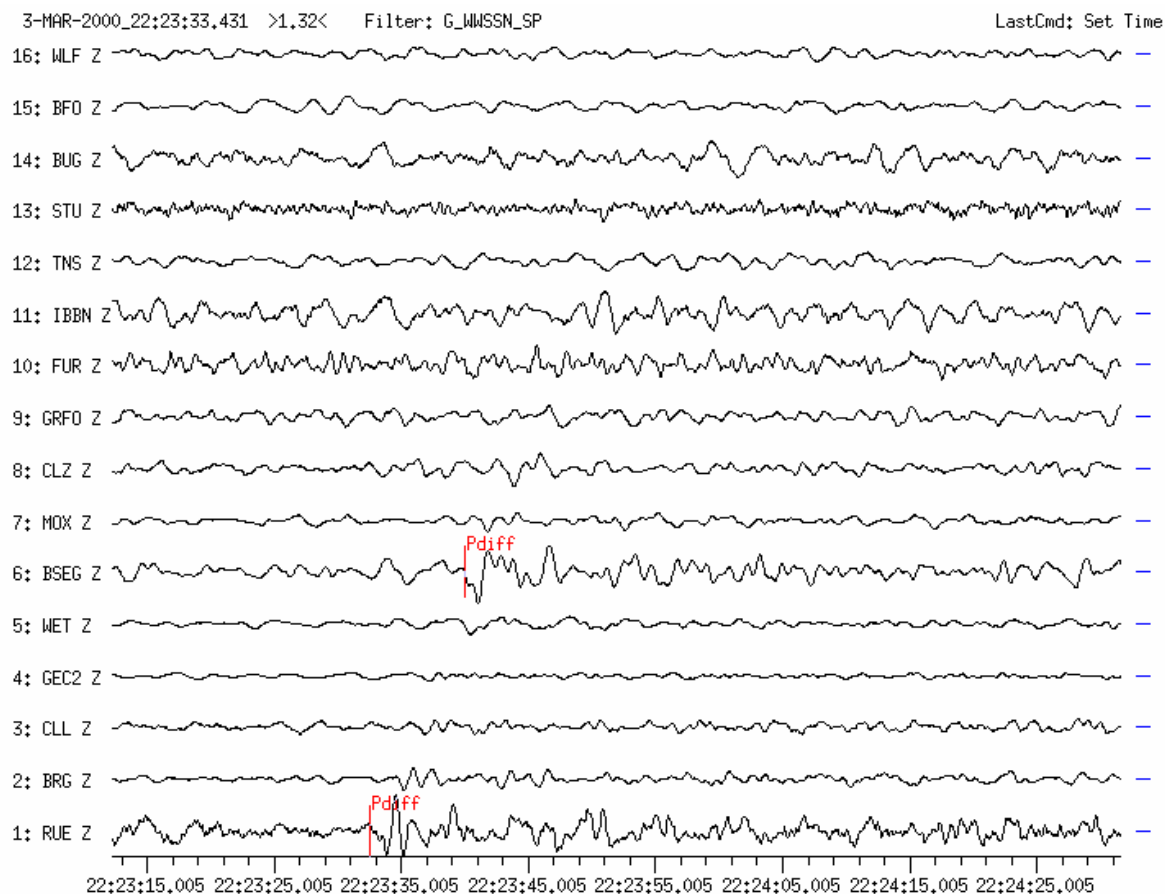


Figure 3a Pdif (old name Pdif) is the first arrival, however, as a diffracted wave, rather small, particularly in short-period records. Only a few GRSN stations have recorded it from this event. For more clear long-period records of Pdif see Figures 4b, 6c and 7b in the next examples.

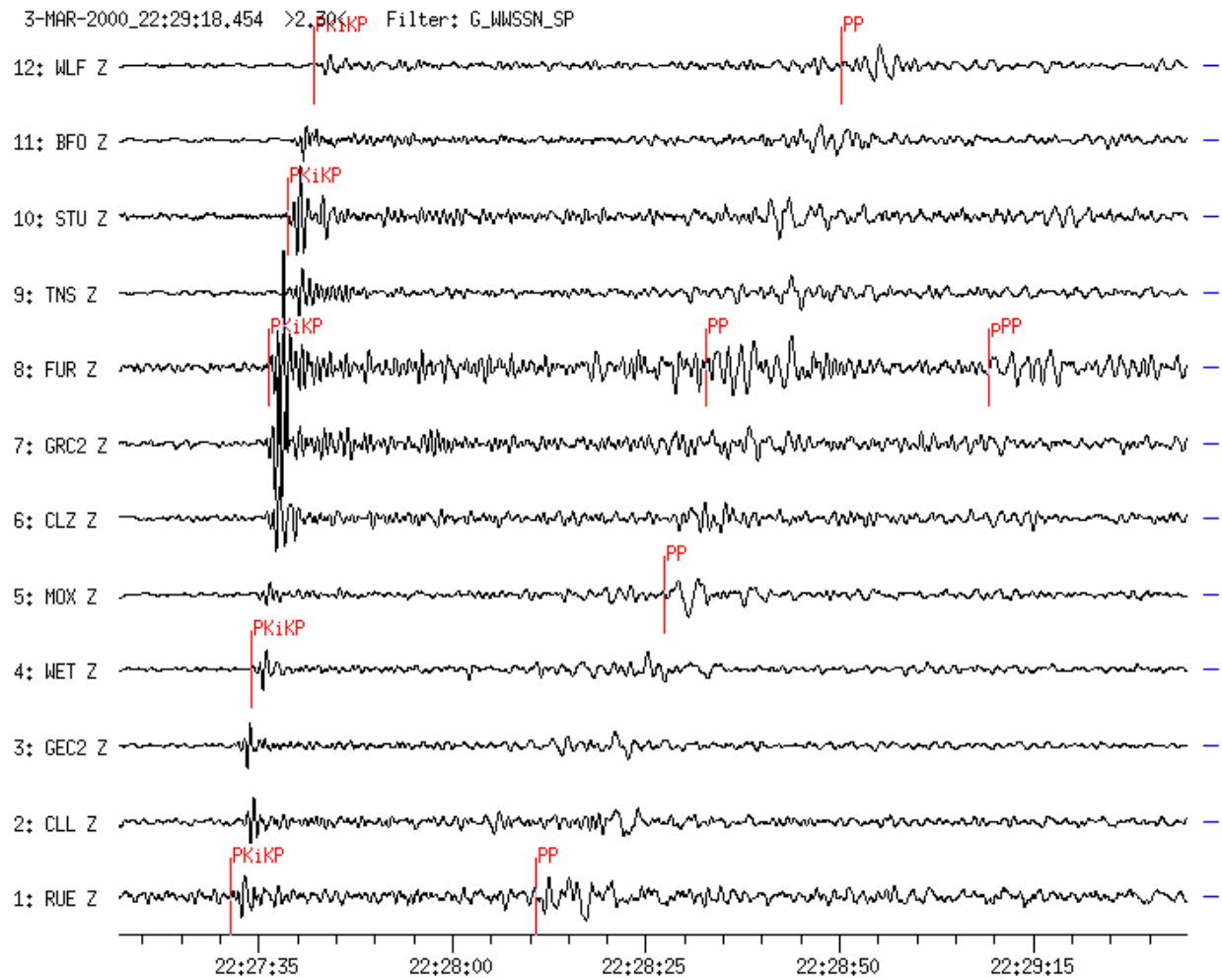


Figure 3b Phases PKiKP, PP and (pPP) are shown on this seismogram. PKiKP arrives about 4 min after Pdif shown in Figure 3a. Note the strong variation at PKiKP-amplitudes within the network by a factor of about 10. The onset-time of PP can not be determined exactly. The reflection point of PP is below the complex crustal structure of Tibet.

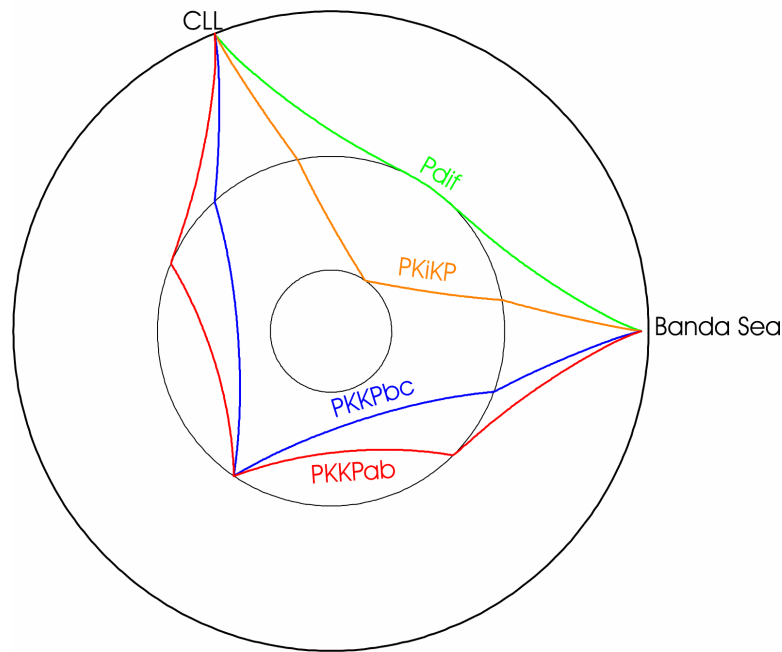


Figure 3c Ray paths for Pdif, PKiKP, PKKPbc and PKKPab for the considered event at a focal depth of 148 km and with an epicentral distance to station CLL of $D = 111^\circ$.

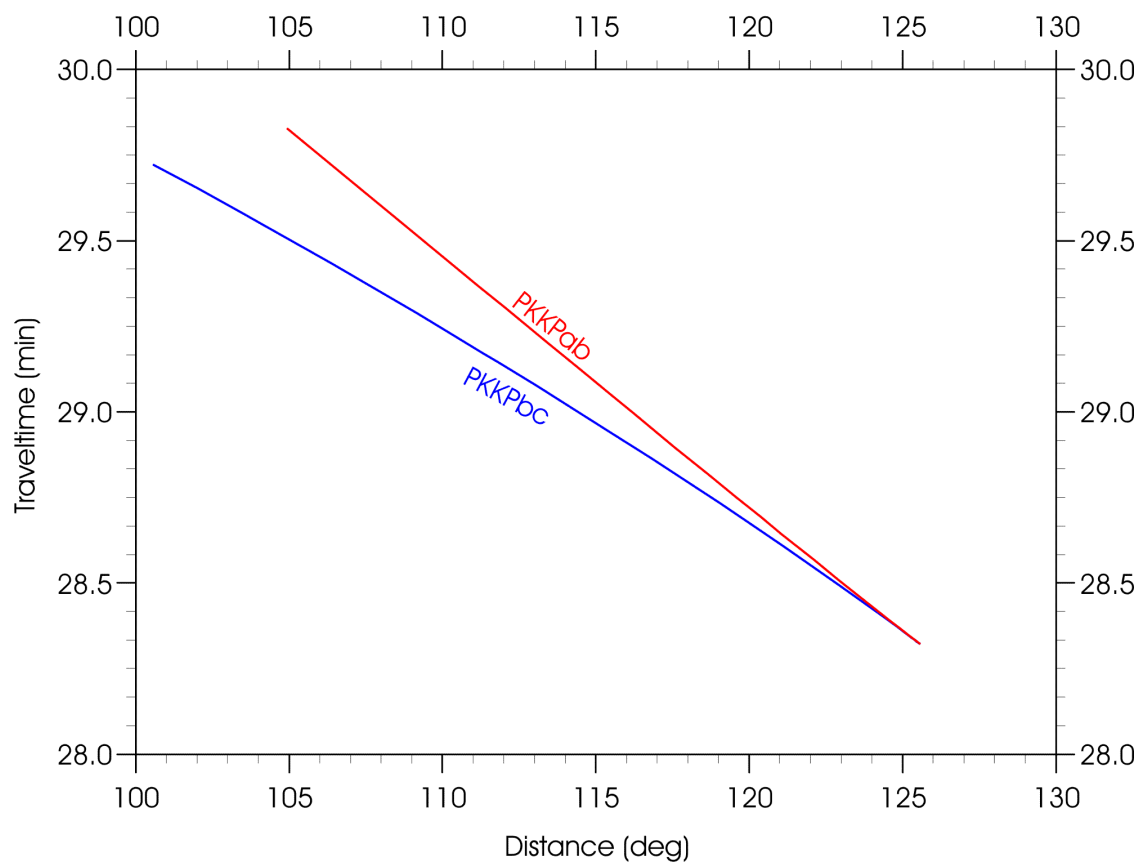


Figure 3d Travel-time curves for PKKPbc and PKKPab for a focal depth of 148 km.

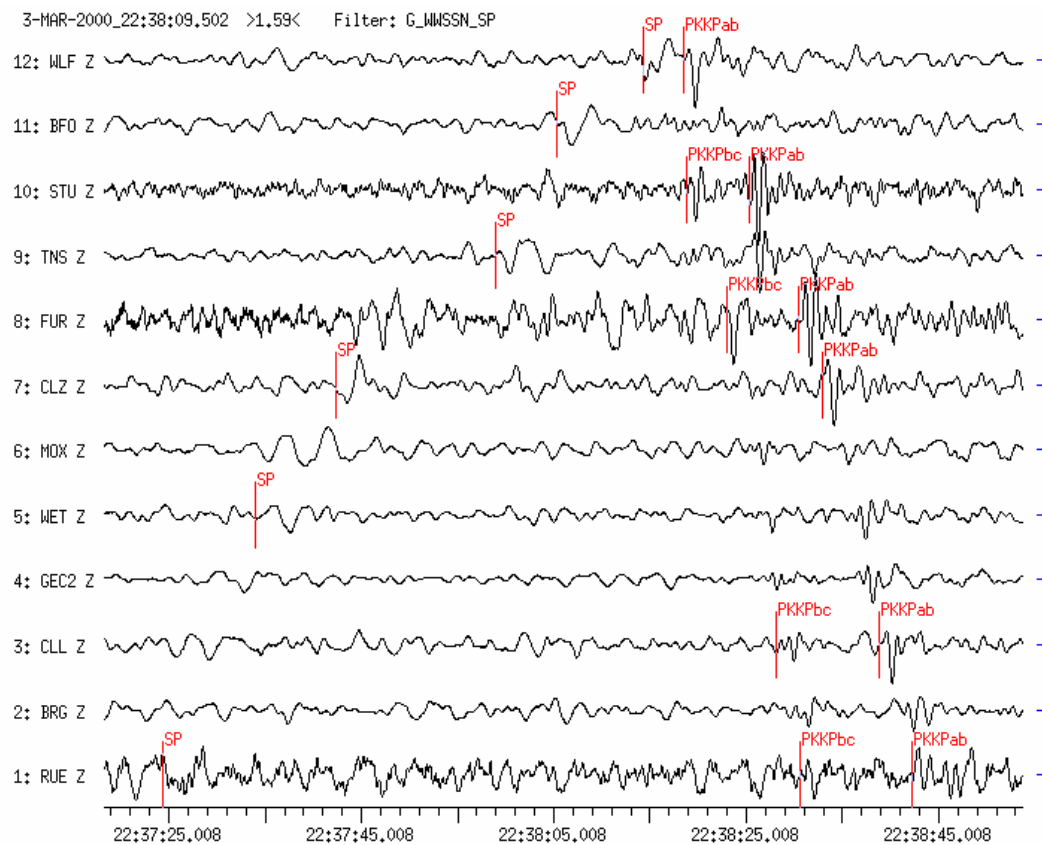


Figure 3e Vertical component short-period seismograms starting about 10 min after the PKiKP arrival in Figure 3b. Marked are the onset times of the phases SP, PKKPbc and PKKPab. For the branching of PKKP between about 90° and 125° see Figure 9 in EX 11.3. These late secondary phases appear in short-period records only. Their ray paths are shown in Figure 3c and their travel-time curves in Figure 3d above.

Example 4: Earthquake in Papua New Guinea

USGS NEIC-data: 1998-07-17 OT 08:49:15 3.08S 141.76E h = 33G Ms = 7.0;
(D = 117.5° and BAZ = 58.8° from GRA1)

This earthquake occurred near the coast of Papua New Guinea. Tsunami waves with a height of 10 m flooded the coast and killed about 3000 people.

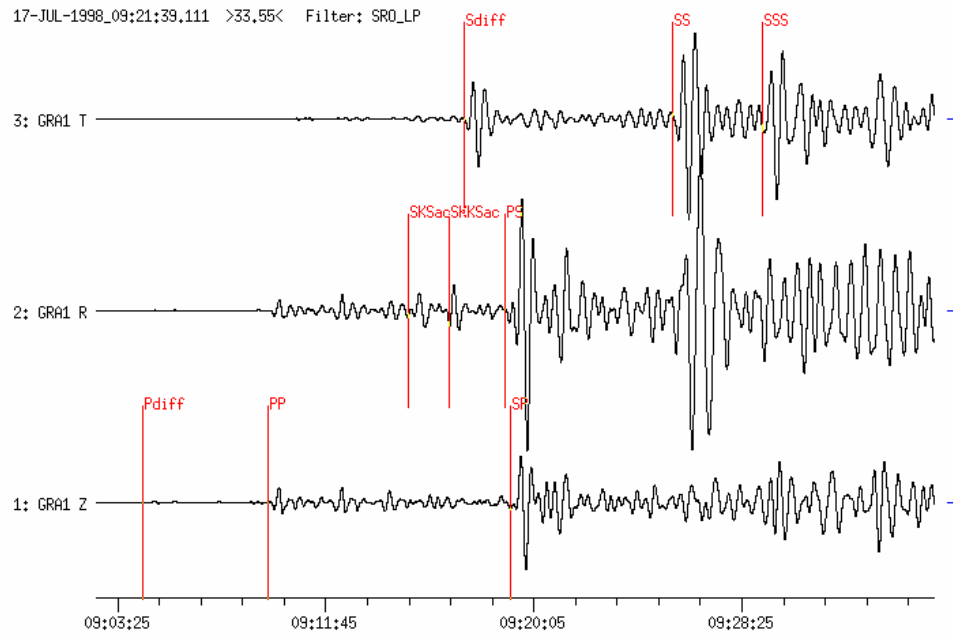


Figure 4a Long-period filtered three-component seismogram (SRO-LP simulation) recorded at station GRA1 ($D = 117.5^\circ$). The horizontal components (RT) are rotated with R into the epicentral direction. Phases Pdif, PP and a strong SP are visible on the vertical component. While the phases SKS, SKKS and PS, polarized in the vertical propagation plane, are strong on the radial (R) component Sdif, SS and SSS are strong on the transverse (T) component.

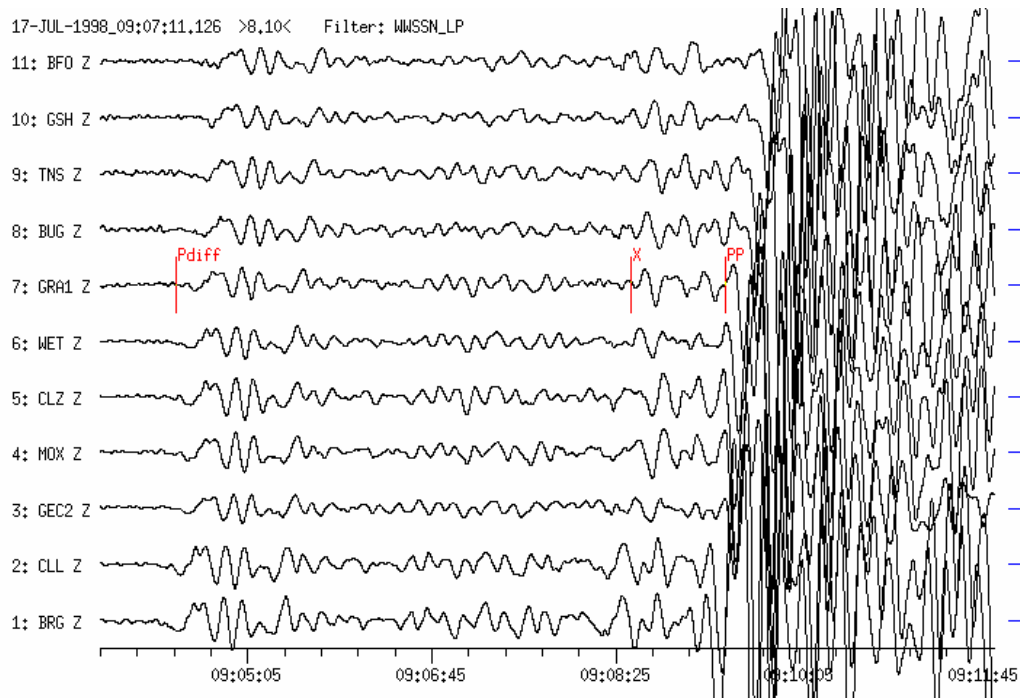


Figure 4b Long-period filtered vertical-component seismograms (WWSSN-LP simulation) recorded at 11 GRSN- and GRF-stations. Traces are sorted according to increasing distance ($D = 115.4^\circ$ to BRG and 119.9° to BFO). Long-period onsets of Pdif and PP are very clear as well as an unidentified phase X ahead of PP. The time differences between X and PP differ from station to station. Probably X results from interfering waves PKPdf and PKiKP. An answer is given in Figure 4c.

Three minutes before the Pdif onset from the earthquake in Papua New Guinea, a small P-wave onset was recorded in the seismograms of GRSN stations from an earthquake in Costa Rica. Its source parameters were:

**USGS NEIC-data: 1998-07-17 OT 08:49:01 8.59N 83.07W h = 33G mb = 5.9;
(D = 86.3° and BAZ = 278.8° from or GRA1)**

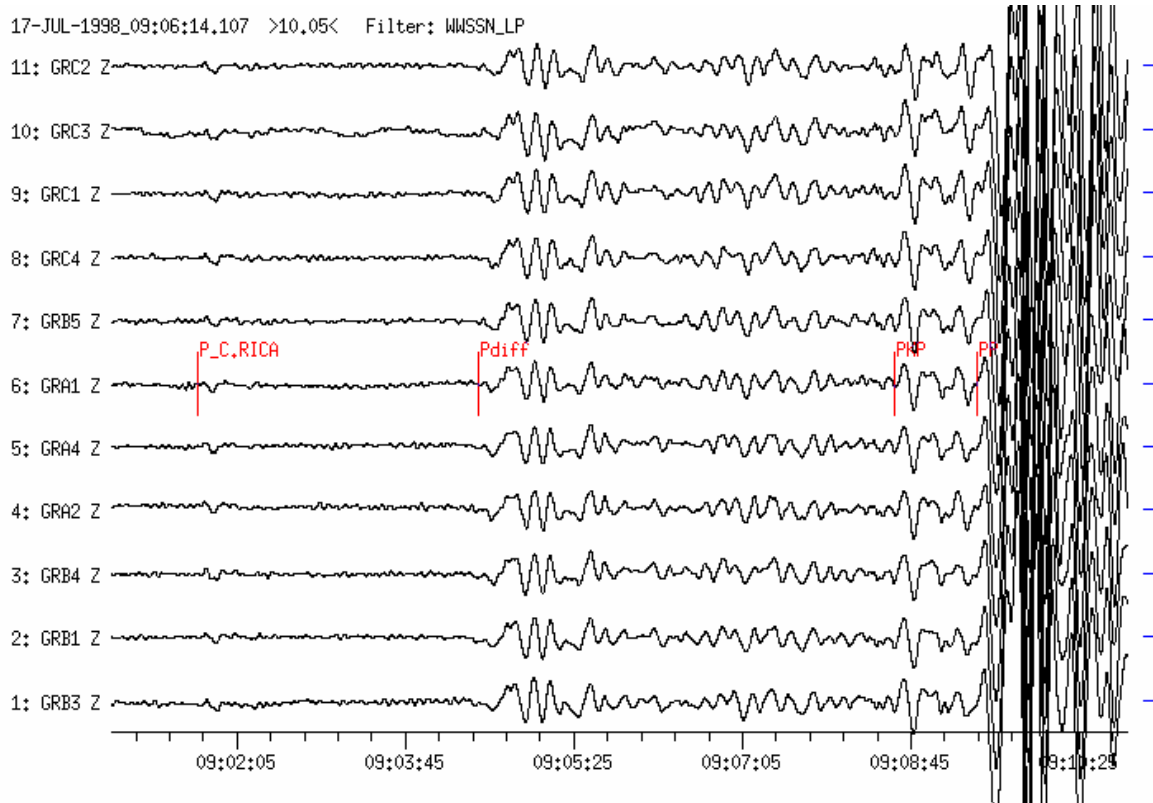


Figure 4c Long-period filtered vertical-component seismograms (WWSSN-LP simulation) recorded at 11 GRF-array stations within the distance range $D = 86.3^\circ$ to 86.7° . Long-period onsets of the P wave from the Costa Rica event appear first, followed by Pdif, PKP and PP from the earthquake in Papua New Guinea. The phase X from Figure 4b could be identified from the GRF-array records as being PKPdf from the Papua New Guinea earthquake with a slowness of about 2.0 s° .

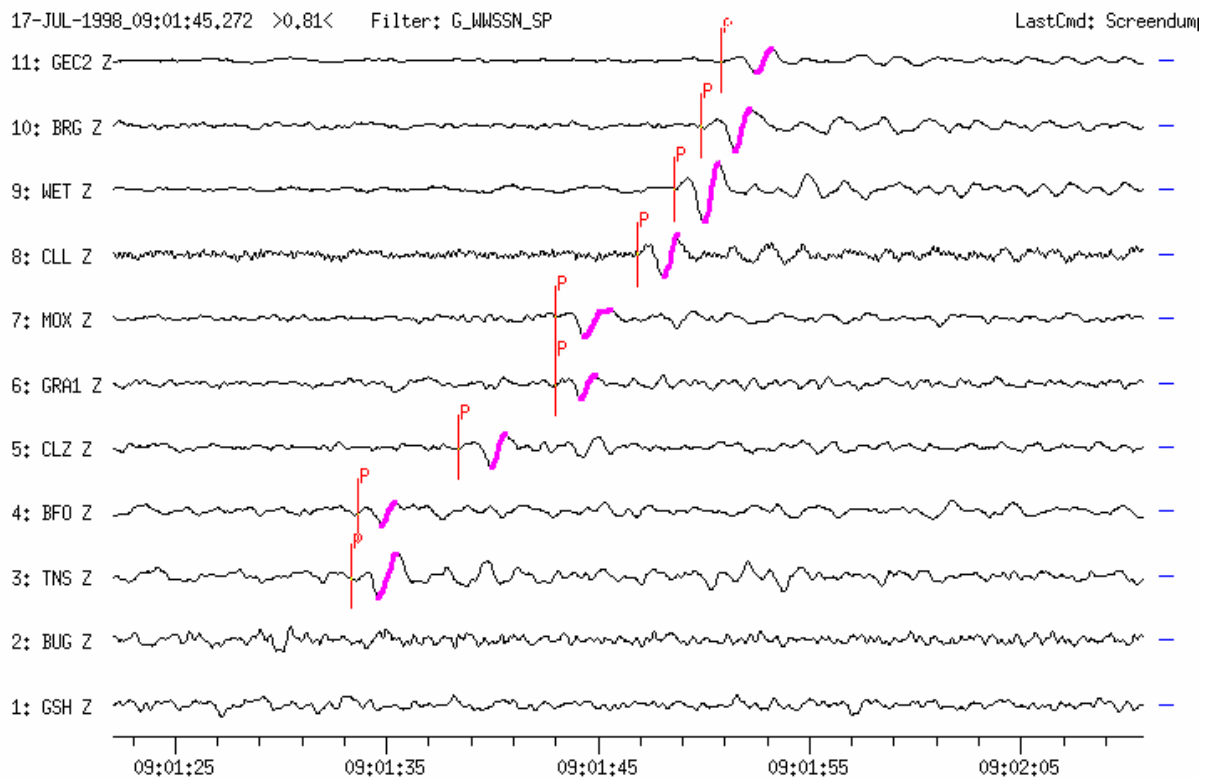


Figure 4d Short-period filtered seismograms (WWSSN-SP simulation) recorded from the Costa Rica earthquake at 11 GRSN-stations. Traces are sorted according to increasing epicentral distance ($D = 83.1^\circ$ to GSH and 88.0° to GEC2). The station-network allows to separate both events by way of slowness and azimuth determination. The estimated body-wave magnitudes m_b vary for the GRSN-stations between values below 5.0 (BUG, GSH) and 5.4 for station WET.

Example 5: Earthquake in the region of New Britain, P.N.G.

**USGS NEIC-data: 1999-05-10 20:33:02.1 5.173S 150.915E $h = 137$ D $m_b = 6.5$;
($D = 124^\circ$ and $BAZ = 51^\circ$ from GRFO)**

This magnitude 6.5 earthquake, recorded at GRFO and at the GRSN-network, shows the phases Pdif, PKP, PP, Sdif, PS, SS, depth phases and – because of a focal depth of 137 km – weak surface waves. A rare example is the well recorded phase P'P'P' = PKPPKPPKPPKPP in Figure 3e below. The ray paths for the identified phases of this event are shown in Fig. 11.60. For animation of ray propagation and seismogram formation see CD-ROM attached to Volume 2 and complementary explanations given in IS 11.3.

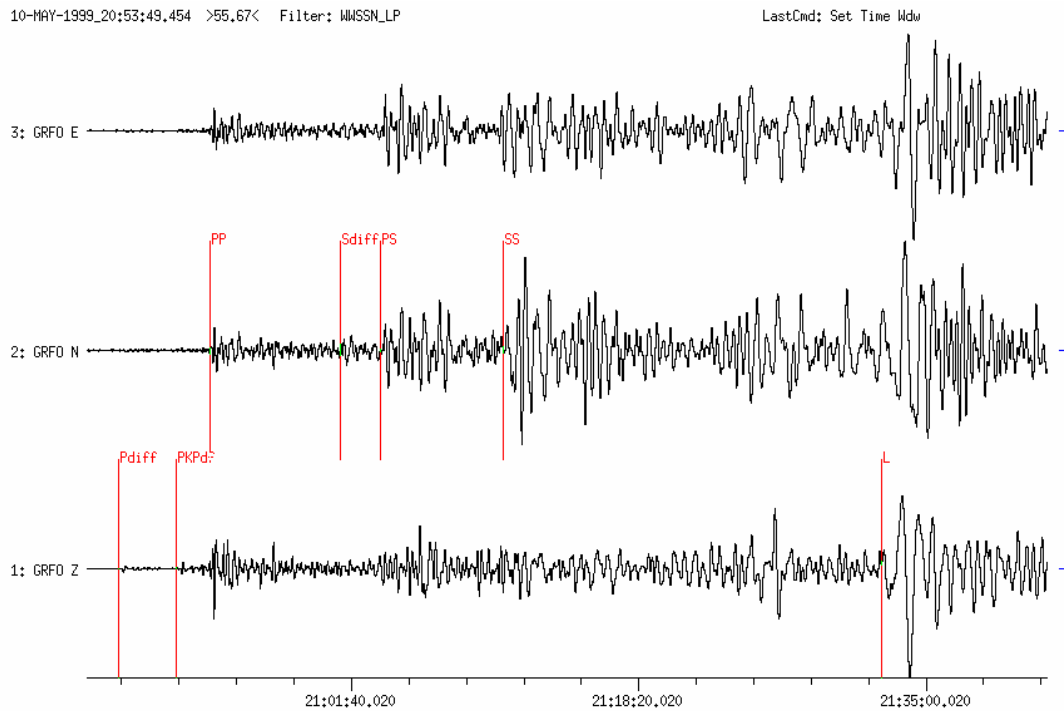


Figure 5a Long-period filtered three-component seismogram (WWSSN-LP simulation) recorded at station GRFO ($D = 124^\circ$). The length of the record is about 1 hour. Phases Pdif, PKP, strong PP, Sdif, strong PS, strong SS and – according to the large focal depth of the earthquake ($h = 137$ km) – relatively weak surface waves are recorded.

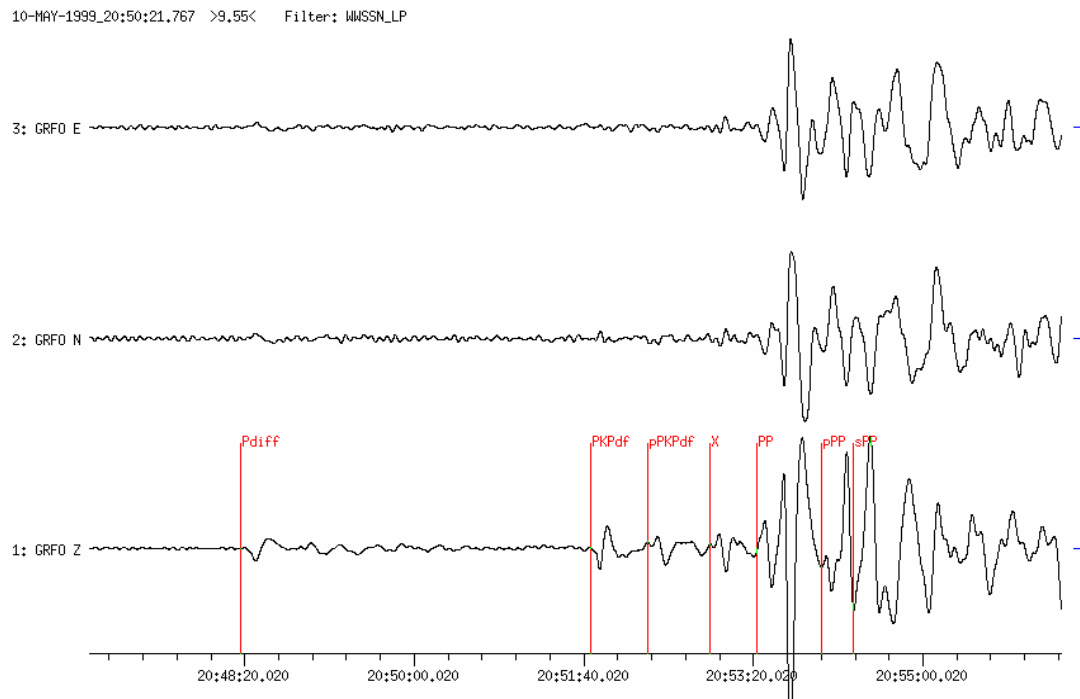


Figure 5b Shown are the first 10 minutes from the seismogram in Figure 5a. The higher time resolution separates well the phases Pdif, PKPd, pPKPd, an unidentified phase X (25s ahead of PP), PP and the depth phases pPP and sPP.

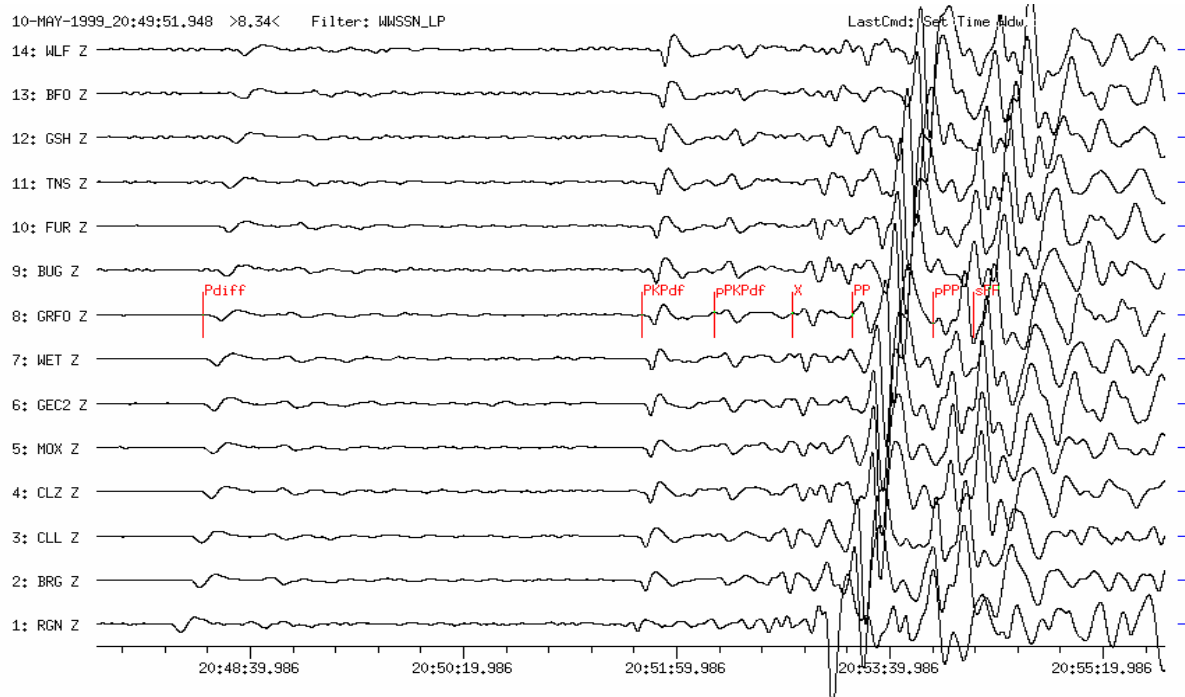


Figure 5c Long-period Z-component records (WWSSN-LP simulation) at 14 GRSN-, GEOFON- and GERESS-stations within the distance range $D = 120.1^\circ$ (RGN) to 126.6° (WLF). This record section was used to perform the vespagram analysis (see Figure5d).

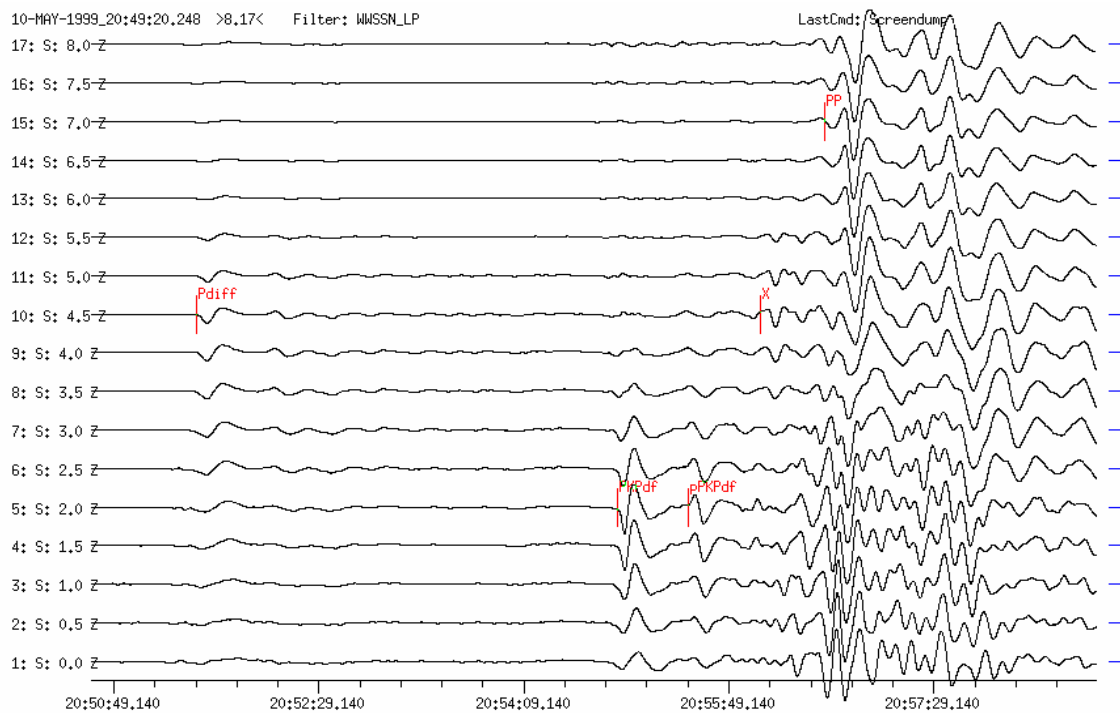


Figure 5d Vespagram analysis for vertical-components was used for slowness determination and phase identification. Phases were identified according to slowness values and travel times. The seismogram analysis program SHM allows to choose slowness steps (here in increments of 0.5 s°). The analysis yields slowness values of 4.5 s° for Pdif, 2.0 s° for PKPdf and pPKPdf, 7.0 s° for PP and for the phase X a value that would correspond to Pdif. The ray path could not be identified.

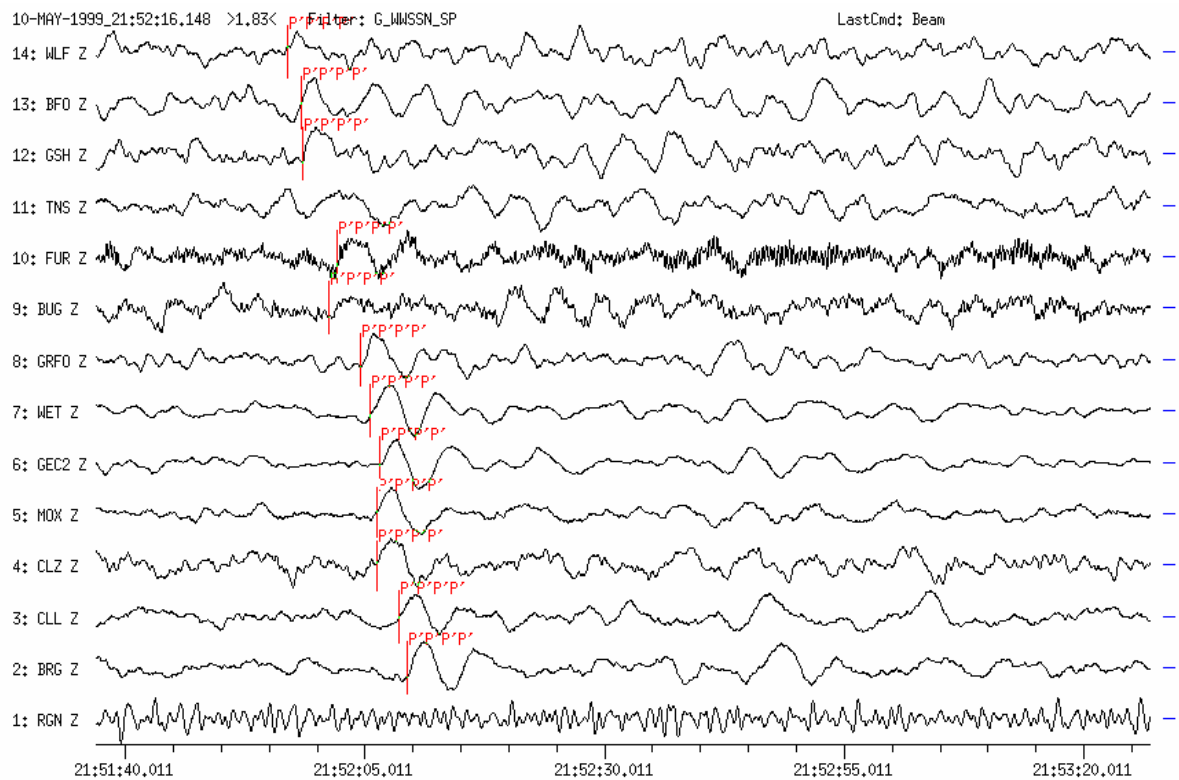


Figure 5e The network records show the rare phase 4P' (PKPPKPPKPPKP) with slowness $S = 2.5 \text{ s}^\circ$. It arrives 79 minutes after the origin time from the opposite azimuth direction (BAZ = 239°).

Example 6: Earthquake in the region of Salomon Islands

USGS NEIC-data: 1996-04-29 OT 14:40:41.2 6.516S 155.037E h = 44G
mb = 6.3 Ms = 7.5;
(D = 127.3 ° and BAZ = 47.5° from GRA1)

The example below presents clear Pdif onsets on long-period filtered seismograms as well as an excellent phase 4P' = P'P'P'P' = PKPPKPPKPPKP arriving about 63 min after the first onset. All records were made at the GRF-array (see Fig. 11.3).

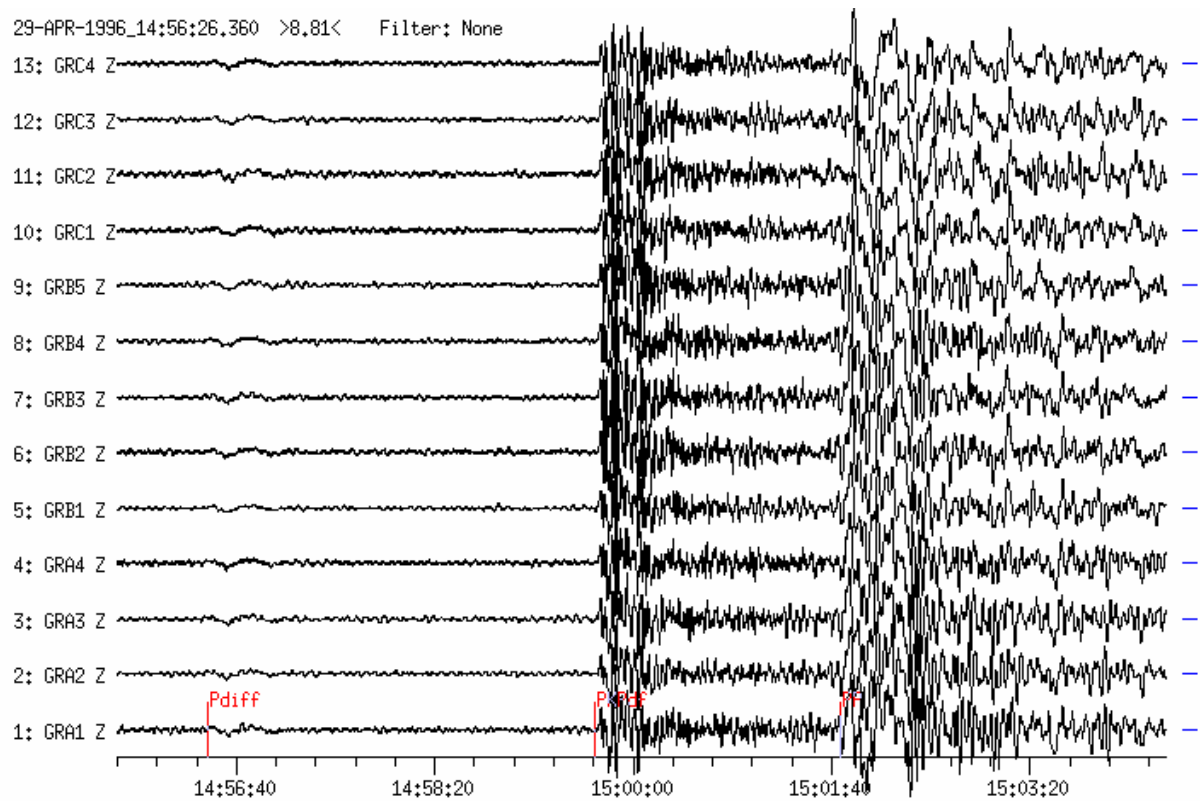


Figure 6a Broadband Z-component records at the GRF array within the distance range $D = 127.2^\circ$ to 127.8° which show, besides the rather long-period Pdif, also PKPdf and PP.

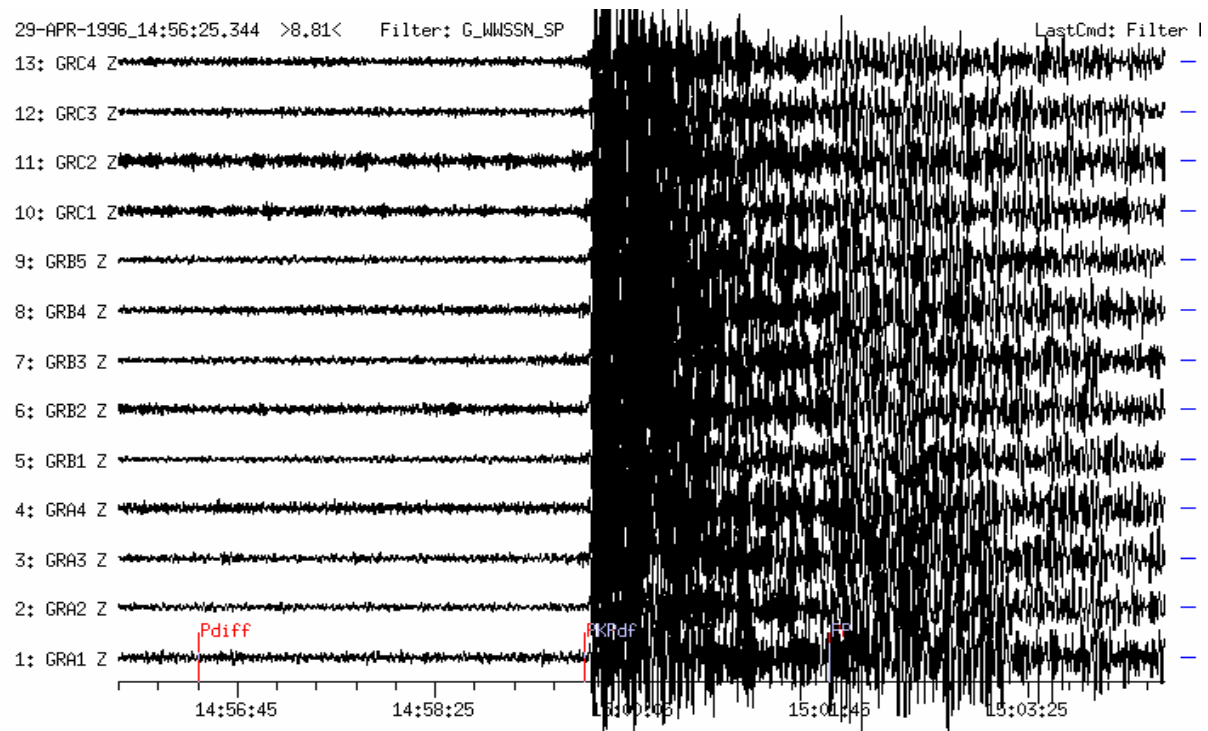


Figure 6b The same record as Figure 6a, however, a short-period filter was applied (WWSSN-SP simulation). Pdif is no longer visible above the noise level.

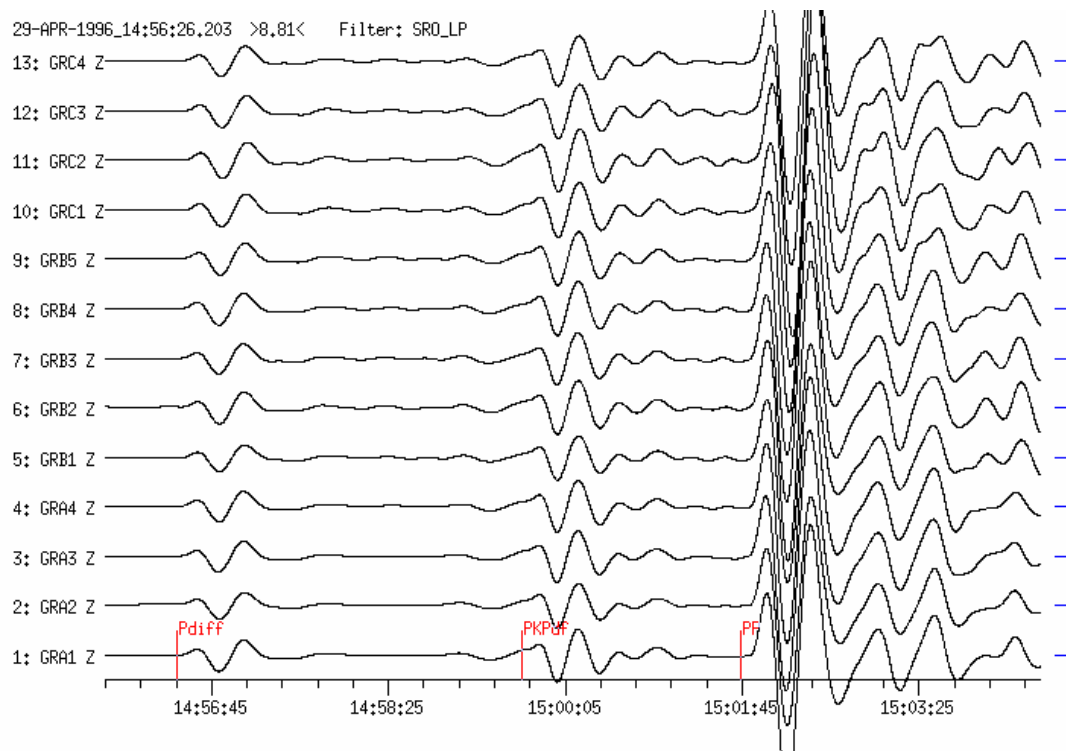


Figure 6c The same records as in Figures 6a and b, however, after applying a long-period filter (SRO-LP simulation). A distinct Pdif appears on the record.

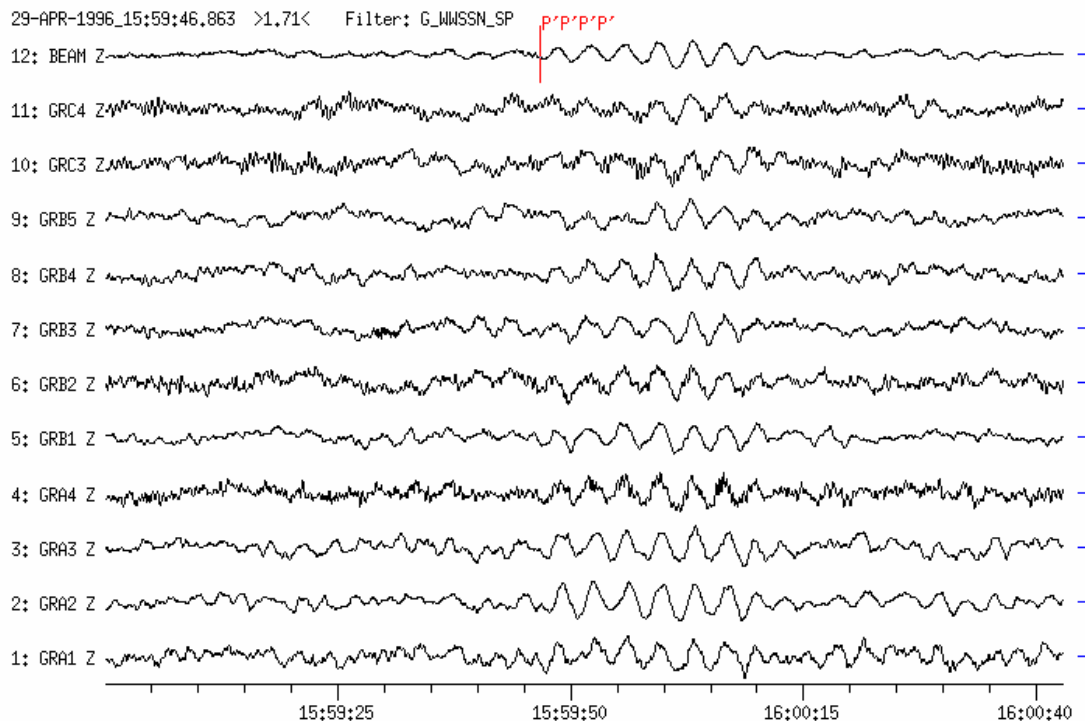


Figure 6d Short-period filtered (WWSSN-SP simulation) seismogram. The rare phase $4P' = P'P'P'P'$ (PKPPKPPKPPK) was clearly recorded at the GRF-array coming from opposite direction (BAZ = 226 and S = 2.56 s/°) about 63 min after the first P onset. Trace No.12 (the sum of all traces = BEAM) shows the best signal-noise-ratio.

Example 7: Earthquake in Santa Cruz Island

USGS NEIC-data: 1998-07-16 OT 11:56:36 11.1S 165.9E h = 110G;
(D = 136.2° and BAZ = 37.3° from GRA1).

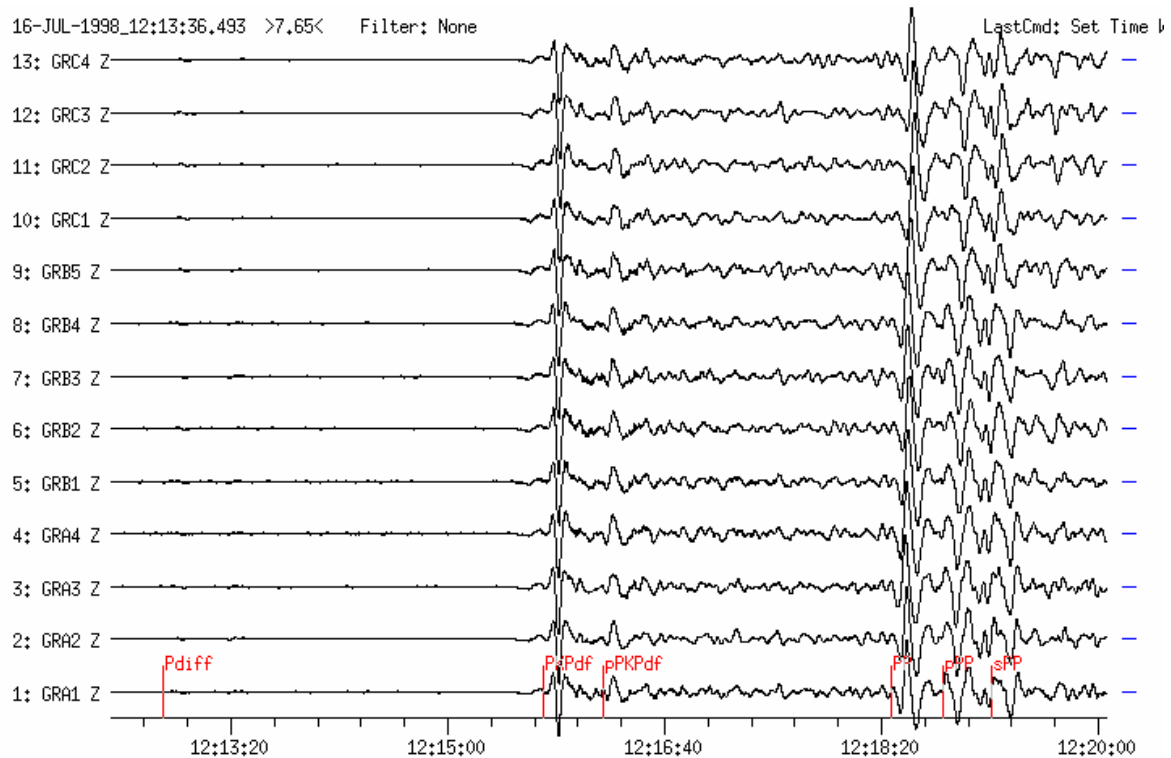


Figure 7a Vertical-component velocity BB seismograms recorded at the GRF-array (distance range between 136.1 and 136.8°). Note the very weak Pdif. The depth phases of PKPdf and PP correspond to a depth of 110 km.

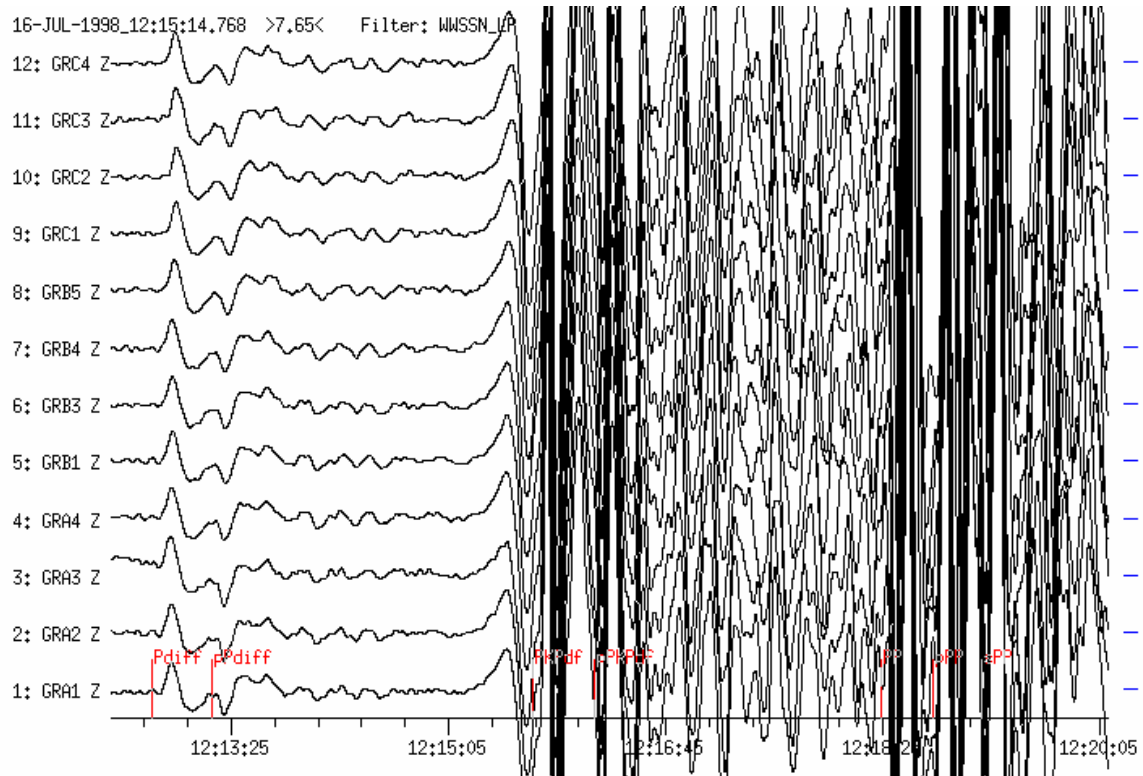


Figure 7b The same record as in Figure 7a, however, after long-period filtering (WWSSN-LP simulation). Note the pronounced onsets Pdif and pPdif. Also remarkable is the long-period and slowly emerging onset 24 sec before PKP.

Example 8: Earthquake in the region of Fiji Islands

USGS-QED-data: 1994-09-30 OT 19:30:06.9 21.102S 179.204W h = 500km(G), mb = 5.1;

The example shows pronounced core phases in the distance range 148° - 152° . Short-period P waves reappear in this distance range but with discontinuous travel-time branches. In the region of the caustic, i.e. around 144° , the whole energy of direct longitudinal core phases is concentrated thus forming a strong PKP onset. Its amplitudes are comparable with that of P waves at much shorter distances (D around 50°). At distances beyond the caustic point PKP onsets are separated into individual PKP branches. The energy distribution changes with increasing distance. PKPbc (or PKP1) is the dominant branch just beyond the caustic, up to about 153° . In records of weaker events, PKPbc is often the first visible onset since PKPdf (or PKIKP), preceding PKPbc, is too weak to be observed. With increasing distance near 160° PKPbc vanishes from the record and PKPab (or PKP2) dominates the seismogram. For more details see sub-section 11.5.2.4.

30-SEP-1994_19:48:50.219 >0.40< Filter: G_WSSN_SP

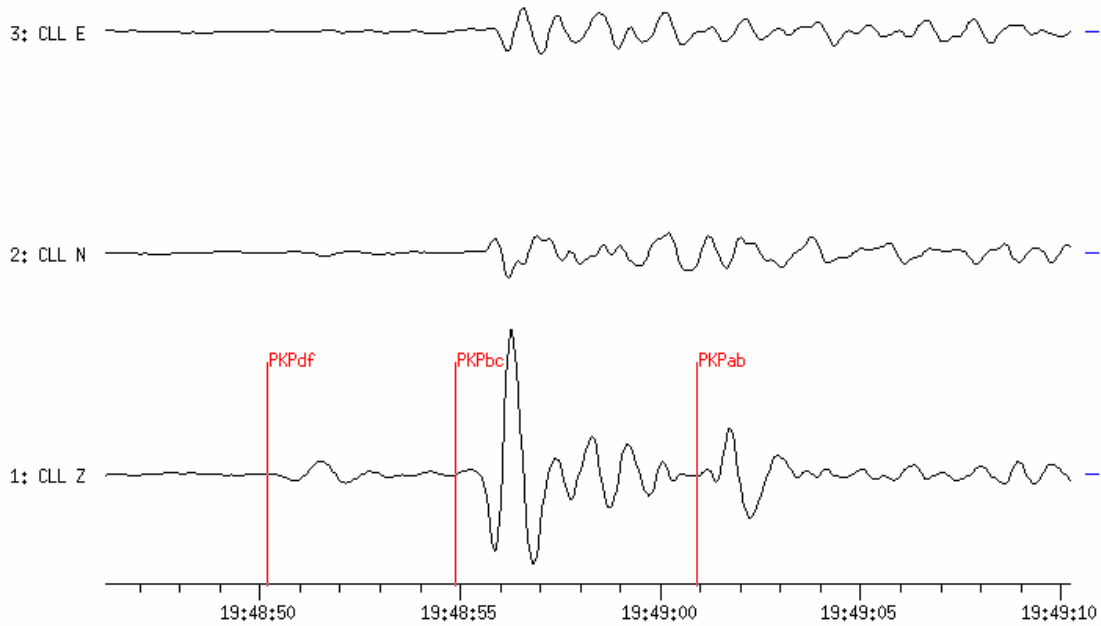


Figure 8a Short-period filtered three-component seismogram (WWSSN-SP simulation) recorded at the broadband station CLL at an epicentral distance of $D = 148.4^\circ$ ($BAZ = 22^\circ$). Phases PKPdf, PKPbc and PKPab are easy to analyse in this distance range. Travel-time curves for the different branches of these core phases allow to determine the epicentral distance from records of a single station only with an error less than 2° . Note the relatively very small amplitudes on the horizontal components because of the very small (steep) incidence angle at this large distance.

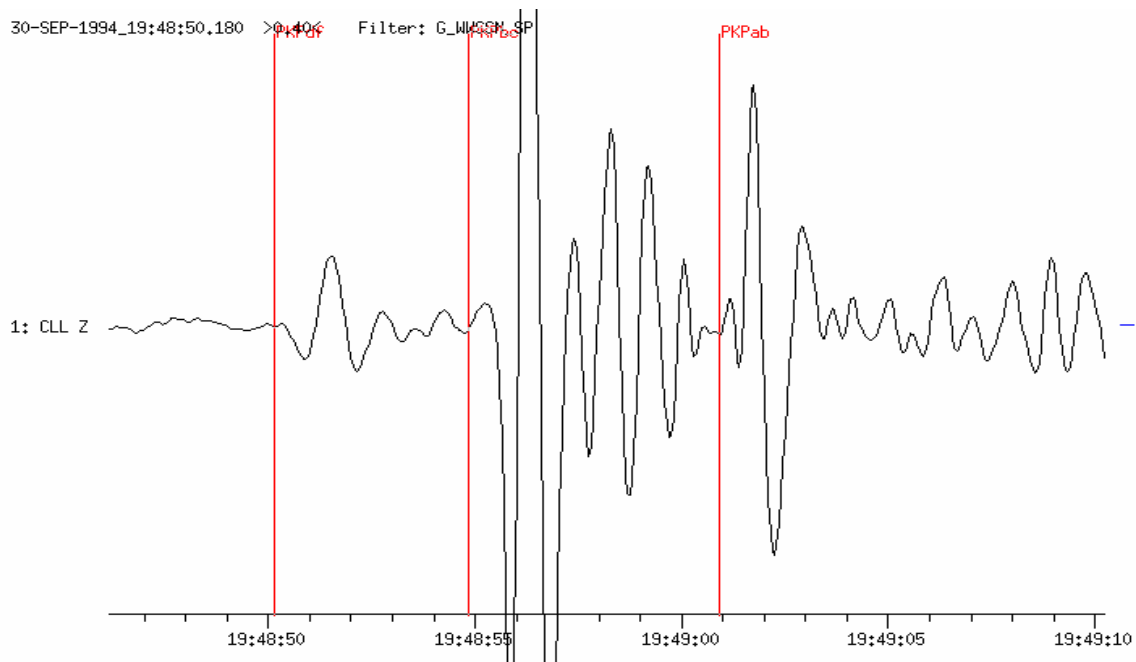


Figure 8b Vertical-component record of station CLL, displayed with higher magnification.

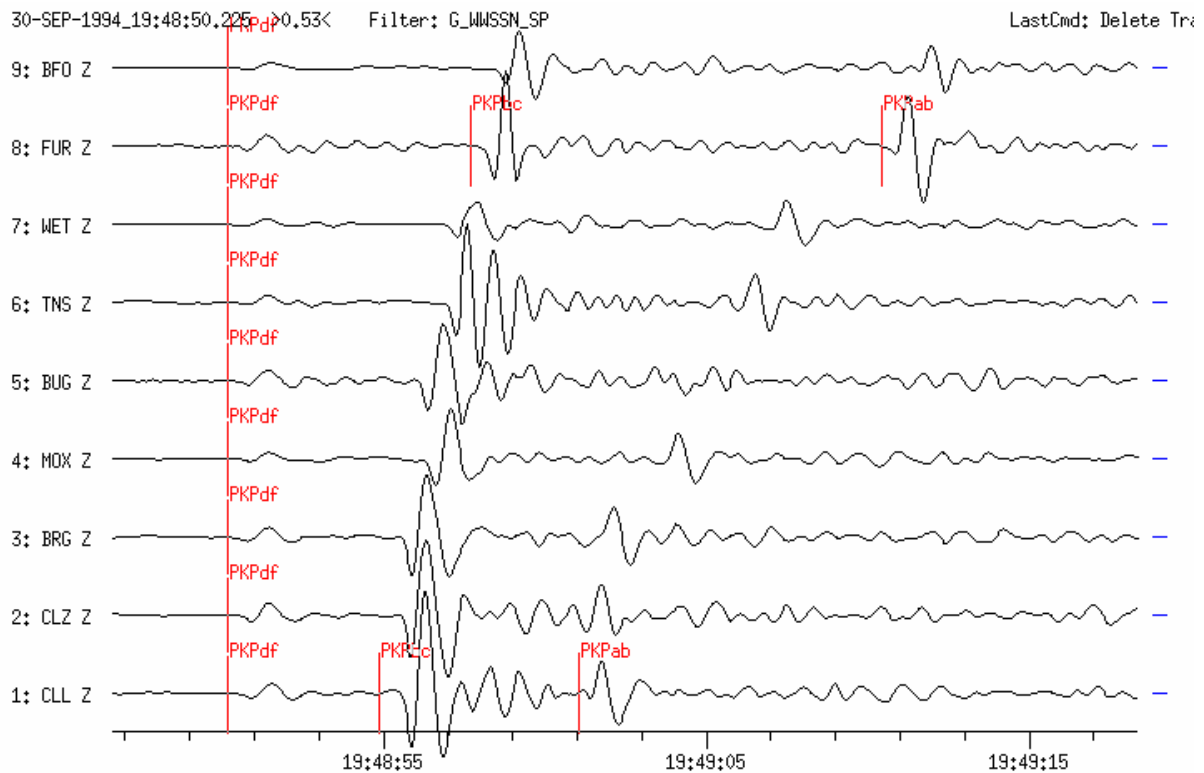


Figure 8c Short-period filtered seismograms (WWSSN-SP simulation) recorded at 9 GRSN-stations. All traces are time-shifted and aligned for PKPdf and sorted according to increasing distance. The epicentral distance for CLL is 148.4° and for the most distant station BFO 152.2° .

Example 9: Deep earthquake in the region of Fiji Islands

USGS NEIC-data: 2000-12-18 OT 01:19:21.6 21.18S 179.12W h = 628 km mb = 6.4;
The epicentral distances of the GRSN stations range between $146^\circ < D < 153^\circ$.

Shown are enlarged cut-outs of the the PKP-wave group from the seismograms presented in Fig. 11.64. The PKP-wave group consists between $146^\circ < D < 156^\circ (160^\circ)$ of three distinct wave arrivals PKPab, bc and df. Fig. 11.59 shows the respective travel-time curves. The figures below demonstrate the effect of the record filter on the discrimination of these closely spaced wave arrivals and the possibility to pick their onset times. The longer the center period of applied narrowband band-pass filters, the worse is the discrimination and onset-time picking for these three core-phase arrivals. Therefore, PKP phases are best picked in SP records, however, the later phases PP and PPP from so distant earthquakes are usually recognizable only in LP or BB records.

2000-12-18 OT 01:19:21.6 $h = 628$ km Fiji Islands region

Z-component, SRO-LP

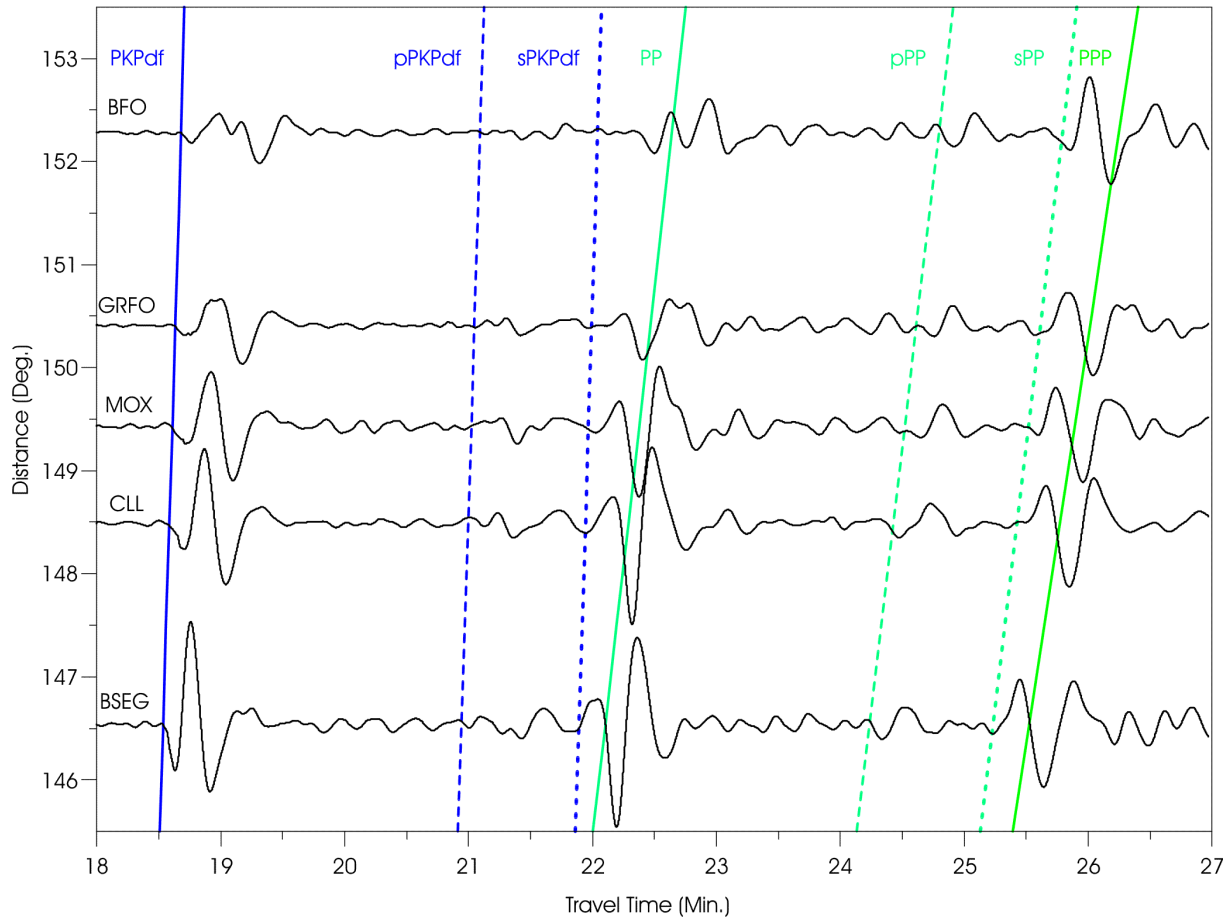


Figure 9a Z component long-period (SRO-LP simulated) records of longitudinal wave groups from a deep ($h = 628$ km) Fiji Islands earthquake at stations of the GRSN. Note the strong onsets of the depth phases sPKPdf and sPPP prior to onsets PP and PPP, respectively, which follow closely.

2000-12-18 OT 01:19:21.6 h = 628 km Fiji Islands region

Model: IASP91 with ellipt. corr.

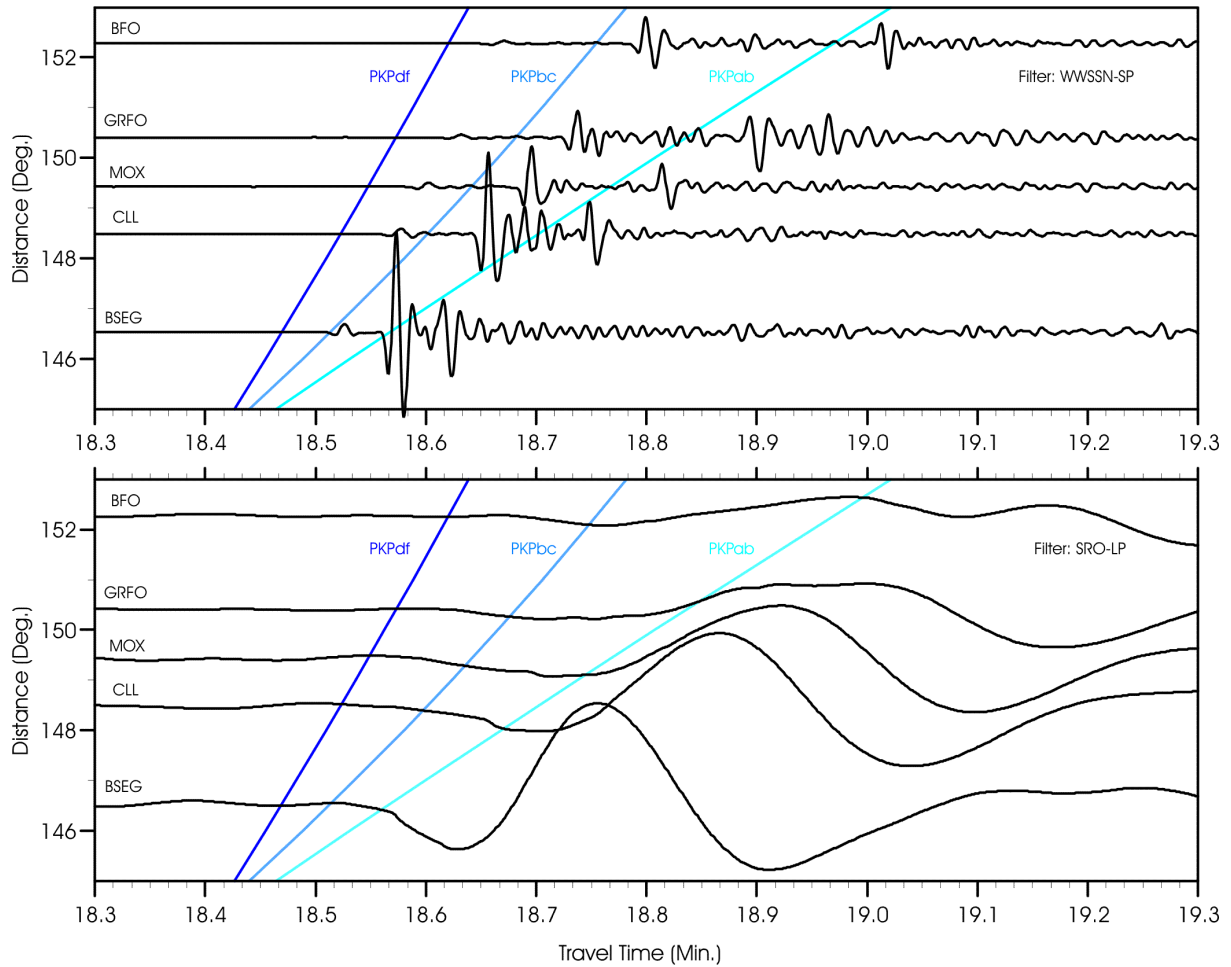


Figure 9b Enlarged cut-outs of the PKP-wave group as recorded in WWSSN-SP (upper traces) and SRO-LP filtered seismograms of the GRSN stations. Note that for all three core phases the theoretically expected onset times according to the IASP91 travel-time model are about 2 s too early.

2000-12-18 OT 01:19:21.6 h = 628 km Fiji Islands region

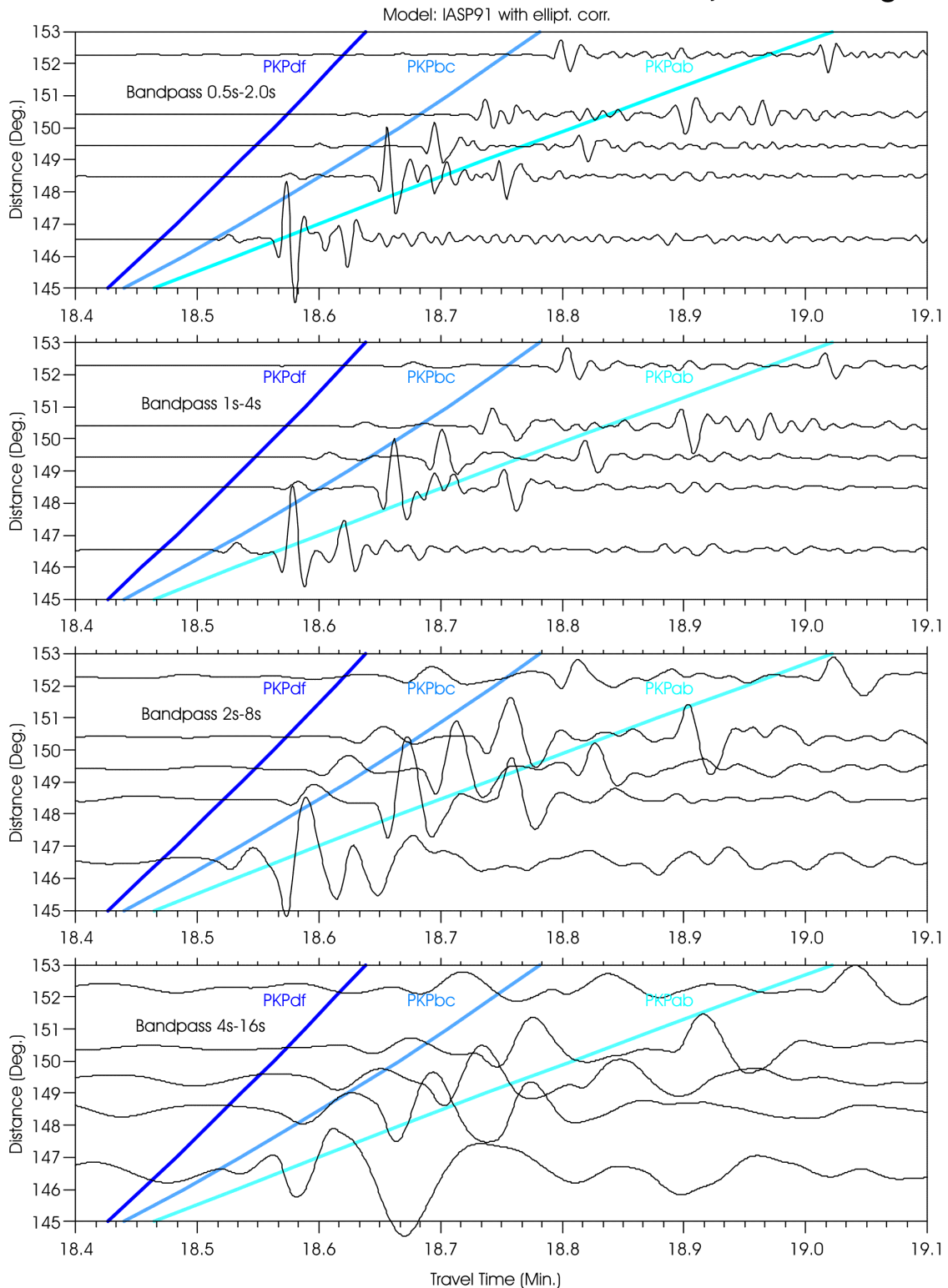


Figure 9c Enlarged cut-outs of the PKP-wave group of the deep Fiji Islands earthquake of 18 December 2000 recorded at stations of the GRSN. Shown are, from top to bottom, the bandpass filtered BB records of two octaves bandwidth with center periods around 1s, 2s, 4s and 8 s. For center periods larger than 3s the separation of the different PKP-wave arrivals and recognition of their onset times becomes less and less clear. Note that according to the IASP91 travel-time model the three core phases should arrive about three seconds earlier.